Clay Minerals (2002) **37**, 607–616

Dedicated to Prof. Dr. U. Schwertmann on the occasion of his 75th birthday

The influence of structural Fe, Al and Mg on the infrared OH bands in spectra of dioctahedral smectites

J. BISHOP[1,*], J. MADEJOVÁ[2], P. KOMADEL[2] AND H. FRÖSCHL[3]

[1] *SETI Institute/NASA-Ames Research Center, Moffett Field, CA 94035, USA,* [2] *Institute of Inorganic Chemistry, Slovak Academy of Sciences, SK-84236 Bratislava, Slovakia, and* [3] *Austrian Research Centers Seibersdorf, Chemical Analytics, A-2444 Seibersdorf, Austria*

(*Received 29 June 2001; revised 14 November 2001*)

ABSTRACT: Visible to near-infrared (NIR) reflectance spectra and mid-IR transmittance spectra are presented here for a collection of dioctahedral smectites. Analysis of the structural OH vibrations is performed by comparing the NIR combination and overtone bands with fundamental stretching and bending absorption features in the mid-IR region. Second derivatives are used to determine the actual band centres, which are often shifted slightly by a spectral continuum in the reflectance or transmittance spectra. New bands have been identified near 4170 and 4000 cm^{-1} in the NIR spectra of nontronite with tetrahedral substitution. A related band is observed near 4100 cm^{-1} for montmorillonites with substantial tetrahedral and/or octahedral substitution. These bands are correlated with the mid-IR bands near 680 cm^{-1} for nontronite and near 630 cm^{-1} for montmorillonite. Comparison of the OH overtone and combination bands with the fundamental stretching and bending vibrations gives consistent results.

KEYWORDS: infrared spectroscopy, smectites, structural OH, montmorillonite, nontronite.

Infrared spectroscopy and other techniques have been employed to understand the structure of iron oxides/oxyhydroxides (Cornell & Schwertmann, 1996; Schwertmann & Cornell, 2000) and phyllosilicates (Farmer, 1974). Iron and other cations have a pronounced effect on the vibrations of OH bonds and can therefore be useful in the characterization of the smectite structure through analysis of visible and infrared spectra.

Mid-infrared spectra of structural OH in dioctahedral smectites

Farmer (1974) summarized the fundamental stretching and bending vibrations due to structural OH in phyllosilicates in the mid-IR region. Dioctahedral smectites include spectral bands due to OH-stretching vibrations (OH_v) near 3630 cm^{-1} for montmorillonite and near 3560 cm^{-1} for nontronite (Farmer, 1974). More recently, detailed analyses have been performed on the specific M_1M_2OH stretching vibrations for $M_{1,2}$ as Al, Fe or Mg in the octahedral cation sites (Madejová *et al*., 1994; Besson & Drits, 1997a,b). Structural OH-bending vibrations (OH_δ) have also been identified for individual pairs of octahedral cations: ~920 cm^{-1} for Al_2OH, ~880 cm^{-1} for $AlFe^{3+}OH$ and ~850 cm^{-1} for AlMgOH in montmorillonite and near 818 cm^{-1} for Fe^{3+}_2OH in nontronite (Stubican & Roy, 1961; Farmer, 1974). Goodman *et al*. (1976) assigned a band near 785 cm^{-1} to $Fe^{3+}MgOH$ bending vibrations and Vantelon *et al*. (2001) attribute the ~850 and

* E-mail: jbishop@mail.arc.nasa.gov
DOI: 10.1180/0009855023740063

818 cm^{-1} bands to $Fe_2^{3+}OH$ bending of OH in *cis* and *trans* groups.

Near-infrared spectra of structural OH in dioctahedral smectites

Spectral bands in the near-infrared (NIR) region result from combinations and overtones of the OH stretching and bending vibrations in dioctahedral smectites. The OH stretching overtone bands are observed near 7090 cm^{-1} (1.41 μm) for montmorillonite and near 7050 cm^{-1} (1.42 μm) for nontronite, while the OH stretching and bending combination bands ($OH_{\nu+\delta}$) are observed near 4530 cm^{-1} (2.20 μm) for montmorillonite and 4370 cm^{-1} (2.29 μm) for nontronite (e.g. Cariati *et al*., 1981; Clark *et al*., 1990; Bishop *et al*., 1993, 1999).

The objective of this study is to compare the spectral features due to structural OH in dioctahedral

TABLE 1. Chemical composition of smectite samples.

	Sampor	Rokle	Pauliberg #751	Steinegg #755	Gossendorf #1565	Landsee #1923	Appersdorf #II3	Gramelkam #4	GSD-1 measured	GSD-1 certified
Major elements (%)										
SiO_2	46.7	45.1	48.3	51.6	53.2	46.5	57.5	56.8	58.8	58.4
TiO_2	0.08	4.46	2.49	0.02	0.35	0.31	0.17	0.10	0.93	0.98
Al_2O_3	2.59	12.8	21.2	1.52	9.78	21.2	16.6	19.2	14.9	14.8
Fe_2O_3	31.6	16.1	8.12	24.4	15.6	5.77	4.85	2.60	7.24	7.35
MgO	0.46	2.80	2.10	4.25	2.26	3.16	3.89	3.71	4.17	4.14
CaO	2.33	2.05	0.93	1.15	2.22	1.19	1.23	1.69	4.44	4.60
Na_2O	0.05	0.11	0.40	1.44	0.25	1.40	0.37	0.18	3.18	3.50
K_2O	0.16	0.77	0.36	0.11	0.53	1.19	0.35	0.14	2.60	2.77
LOI	15.8	14.7	14.9	12.4	14.9	16.1	14.4	15.2	2.78	>2.16*
Trace elements (ppm)										
Li	3	14	52	6	37	120	22	16	33	29.6
Be	1.2	3.7	2.5	1.0	4.5	2.2	3.4	3.8	3.3	3
V	43	420	168	37	162	110	28	21	128	121
Cr	20	109	410	1570	125	55	17	8	193	194
Mn	22	1800	450	850	460	600	112	122	940	900
Co	0.5	58	53	134	19	7	3	4	22	20.4
Ni	4	59	600	4500	57	42	12	12	82	76
Cu	121	390	390	18	51	67	16	12	23	21.8
Zn	80	130	120	53	130	88	76	47	84	79
Ga	4	26	37	2	14	23	23	24	23	23
As	31	3	1	1	7	5	4	<1	1	1.96
Rb	10	39	77	8	72	53	24	11	120	116
Sr	48	250	85	20	165	90	65	165	550	525
Zr	130	360	330	<50	120	<50	190	105	300	310
Nb	<10	12	44	<10	10	29	22	17	36	35
Mo	0.23	5.33	1.23	0.12	1.62	2.24	0.41	0.44	0.72	0.74
Cd	<0.1	0.7	0.4	0.2	0.2	0.4	0.2	0.3	0.2	0.088
Sb	0.34	0.66	0.81	0.45	0.70	0.95	1.18	1.23	0.24	0.22
Ba	450	510	118	27	170	350	73	42	980	950
Tl	0.16	0.20	0.23	0.09	3.34	0.37	0.17	0.10	0.66	0.61
Pb	4.6	11	11	4.6	16	44	22	43	28	24.4
Bi	0.7	0.2	0.4	<0.1	1.1	0.3	0.6	0.6	0.6	0.66
U	2.1	1.9	2.3	0.3	7.1	3.3	6.6	4.1	4.7	4.4
Total	99.87	99.31	99.10	97.61	99.25	96.99	99.43	99.69	99.40	96.79

The major elements were determined using XRF; the trace elements were determined using ICP-MS, except for Zn, Zr and Nb which were determined using XRF; loss on ignition (LOI) was determined at 850ºC; GSD indicates geological standard; *LOI not determined for GSD-1, but H_2O was measured at 2.16%.

TABLE 2. Structural composition of smectite samples in this study (per $O_{20}(OH)_4$).

Sample	Origin	Octahedral cations Al	Fe	Mg	Tetrahedral cations Si	Al	Fe	Interlayer cations (M^+)	Admixtures
Jelšový Potok*	Slovak Rep.	2.99	0.38	0.63	7.70	0.30		0.93	~3% SiO_2 (IR), ~50% Fe_2O_3 as Gt (MB/VIS)
Sampor[+]	Slovak Rep.		3.91	0.09	7.03	0.61	0.36	0.97	
Rokle[‡]	Czech Rep.	2.01	1.64	0.35	6.87	1.13		1.50	~50% Fe_2O_3 as Gt (MB)
Stebno[¶]	Czech Rep.	1.96	1.60	0.58	7.22	0.78		0.95	~3% kaol (IR), ~20% Fe_2O_3 as Gt (MB/VIS)
SAz-1[#]	CMS	2.67	0.15	1.20	8.00			1.11	
SWa-1*,[+]	CMS	0.84	2.93	0.28	7.27	0.73		0.81	
SWy-1*	CMS	3.07	0.44	0.54	7.66	0.34		0.74	
Pauliberg	Austria	3.40	0.11	0.56	7.78	0.22		0.58	~10% kaol (IR), ~90% Fe_2O_3 as Hm (VIS)
Steinegg	Austria	0.25	2.84	0.98	7.97	0.03		0.83	trace Qtz (IR)
Gossendorf	Austria	1.74	1.62	0.52	7.98	0.02		0.89	~2% SiO_2 (IR), ~10% Fe_2O_3 as Gt (MB)
Landsee	Austria	2.64	0.73	0.83	7.04	0.96		1.21	~15% kaol (IR), ~5% Fe_2O_3 as Gt (VIS)
Appersdorf	Germany	2.79	0.48	0.83	7.99	0.01		0.54	~3% Qtz/SiO_2 (IR), ~9% Fe_2O_3 as Hm (MB)
Gramelkam	Germany	3.06	0.28	0.80	7.79	0.21		0.60	~5% SiO_2

The cation compositions have been determined by adjusting the results of the chemical analyses (from Table 1 or other studies) for known admixtures identified through IR or Mössbauer (MB); the iron oxide minerals goethite (Gt) and hematite (Hm) are given relative to the total Fe in the sample, with the assumption that the remaining Fe is in the smectite structure; the abundance of quartz (Qtz), amorphous silica (SiO_2) or kaolinite (kaol) admixtures is given as % of total sample; the interlayer cations are primarily Ca for these samples, except for Steinegg and Landsee which have both Ca and Na; *data from Madejová *et al*. (1994); [+]data from Bishop *et al*. (1999); [#]data from Breen *et al*. (1995); [¶]data from Čičel *et al*. (1992a); [‡]data from Čičel *et al*. (1992b).

smectites that are found in the NIR and mid-IR regions. Because the vibrations of the OH-stretching and bending bands vary slightly depending on the octahedral cations bound to the hydroxyls it is useful to analyse montmorillonites and nontronites that have different octahedral cation site occupancies. NIR reflectance spectra and mid-IR transmittance spectra of several Fe-bearing dioctahedral smectites are presented here and spectra of the OH combinations and overtones are used to help explain the influence of cations, especially Fe, on the fundamental OH-bending and stretching vibrations.

METHODS

Samples

Smectite samples studied here were either obtained from the Clay Minerals Society (CMS), Source Clay Minerals Repository, or were collected in the Czech Republic, the Slovak Republic, Austria or Germany (lower Bavaria). The Appersdorf and Gramelkam samples are from southern Bavaria and developed through alteration of glassy volcanic ash that originated in the Pannonian basin (Hungary) ~14–15 million years ago. The sample from Steinegg was collected in a region dominated by granulitic rocks and the sample from Landsee is a weathering product of Palaeozoic mica schists. The Pauliberg and Gossendorf smectites were formed through weathering of basaltic rocks in the volcanic region of Styria. Chemical analyses have been performed on the smectites from the CMS collection (Madejová *et al*., 1994; Breen *et al*., 1995; Bishop *et al*., 1999) and Czech or Slovak Republics (Čičel *et al*., 1992a,b; Madejová *et al*., 1994) in previous studies. New chemical analyses of the smectites in this study were determined

through XRF and ICP-MS as in other studies (e.g. Bishop *et al*., 2001) and are reported in Table 1. The sample names and places of origin are listed in Table 2. All samples have been purified via sediment fractionation to <2 μm particle size.

Many of the samples selected for this study have high Fe abundances because we are particularly interested in smectites with structural Fe. Whenever possible any iron oxide minerals present were identified through a variety of techniques and listed in Table 2. High Ni, Co and Cr values in the Pauliberg and Steinegg samples and the high Cu value in the Pauliberg sample suggest a basaltic/ultra-alkaline origin for these clays. The high trace element abundances are thought to be present in both the smectites and accessory minerals in these samples.

The octahedral site occupancy was determined as described by Číčel & Komadel (1994) from the chemical composition with consideration of possible impurities determined through XRD, visible, IR and Mössbauer spectral measurements. The octahedral and tetrahedral cation compositions for the smectites in this study are listed in Table 2 along with approximate admixture components.

Transmittance spectroscopy

Infrared transmittance spectra were recorded using a Nicolet Magna 750 FTIR spectrometer. Each spectrum consists of 256 scans at a resolution of 4 cm^{-1}. Aliquots of 0.4 mg of sample were added to 200 mg of KBr to form pressed pellets using standard procedures (e.g. Madejová *et al*., 1994). Samples were prepared directly prior to measurement in order to minimize adsorption of atmospheric water.

Reflectance spectroscopy

Reflectance spectra were measured of undiluted powders in a horizontal sample dish using a bi-directional visible/near-infrared spectrometer and a Nicolet FTIR spectrometer as in previous studies (Bishop *et al*., 1994, 1999). Spectra were measured relative to Halon from 0.3 to 3.6 μm under ambient conditions. Infrared reflectance spectra were measured relative to a rough gold surface in an H_2O- and CO_2-purged environment. Composite, absolute reflectance spectra were prepared by scaling the FTIR data to the bidirectional data near 1.2 μm.

RESULTS

Reflectance spectra and their second derivatives are shown in Fig. 1 for two smectites in the NIR region. In order to determine the band centres for spectral absorptions it is convenient to remove the spectral continuum around the band of interest or to use the second derivative. The OH-combination bands due to montmorillonite and nontronite are indicated in Fig. 1 for the reflectance and second derivative data in order to illustrate the utility of this method.

Structural OH-bending and stretching vibrations

Transmittance spectra of the smectites in this study are shown in Figs 2 and 3 for the OH-bending and stretching regions, respectively. Second derivatives of these spectra were used in most cases to determine the band centres, which are summarized in Table 3. In addition to the spectral features due to vibrations of the bonds in the smectite structure, some samples exhibit bands near 795 cm^{-1} due to silica, a doublet at ~780 and 798 cm^{-1} due to quartz, or bands near 670, 700, 750, 3625, 3700, 7225 and 7255 cm^{-1} due to kaolinite-serpentine group clays. It is difficult to select the OH_ν bands from second derivatives for smectites because of the multiple, overlapping stretching vibrations of both the structural OH and bound water; thus, the OH_ν bands given in Table 3 are the band centres measured from the transmittance spectra of the composite OH_ν bands.

Comparison of near-infrared and mid-infrared OH bands

Reflectance spectra of the smectites in this study are shown in Fig. 4 for the OH combination region. $OH_{\nu+\delta}$ bands are observed for the FeFeOH sites near 4370−4380 cm^{-1}, for the AlFeOH sites near 4465−4475 cm^{-1} and for the AlAlOH sites near 4525−4535 cm^{-1} (Table 3). The exact position of the band centre depends on the distribution of Al, Fe and Mg octahedral cation pairs. The Sampor and Steinegg samples exhibit nontronite-OH combination bands, while Stebno, SWa-1 and Gossendorf exhibit OH-combination bands characteristic of both Al and Fe in octahedral sites. Samples JP, SWy-1, Appersdorf, Gramelkam, Landsee and Pauliberg exhibit $OH_{\nu+\delta}$ bands consistent with mostly Al in

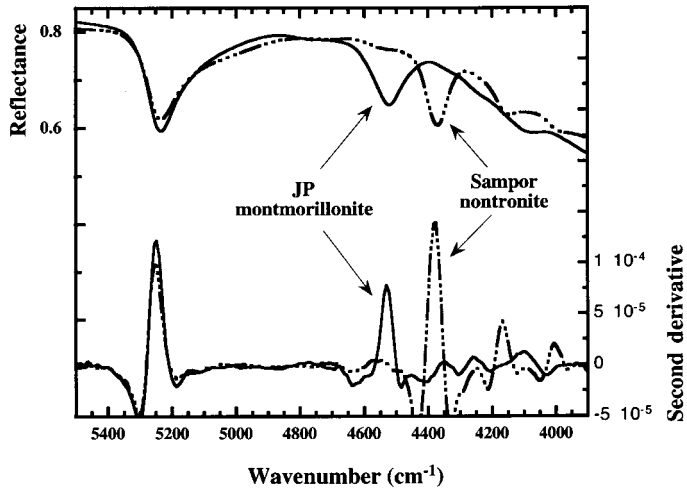

FIG. 1. Reflectance spectra of two smectites in the NIR region and second derivatives of these spectra. Second derivatives of reflectance and transmittance spectra can be used to remove the spectral continuum and locate the band centre. Spectra of the Jelšový Potok (JP) montmorillonite are shown by the solid black line; those for the Sampor nontronite are shown by the broken line.

the octahedral sites, while the Rokle smectite exhibits spectral bands due to substantial Fe as well as Al, and SAz-1 has a band shifted toward the AlMgOH character. An OH-combination band is also observed in this region for kaolinite (see Fig. 3 in Bishop *et al*., 2002, this issue). This kaolinite feature is characterized by a combination of a sharp band at 4530 cm^{-1} and a broad band near 4630 cm^{-1} and overlaps with the smectite features near 4600 cm^{-1} in the Landsee spectrum (Fig. 4b).

Additional bands are observed at 4165 and 4005 cm^{-1} for the Sampor nontronite. Previously,

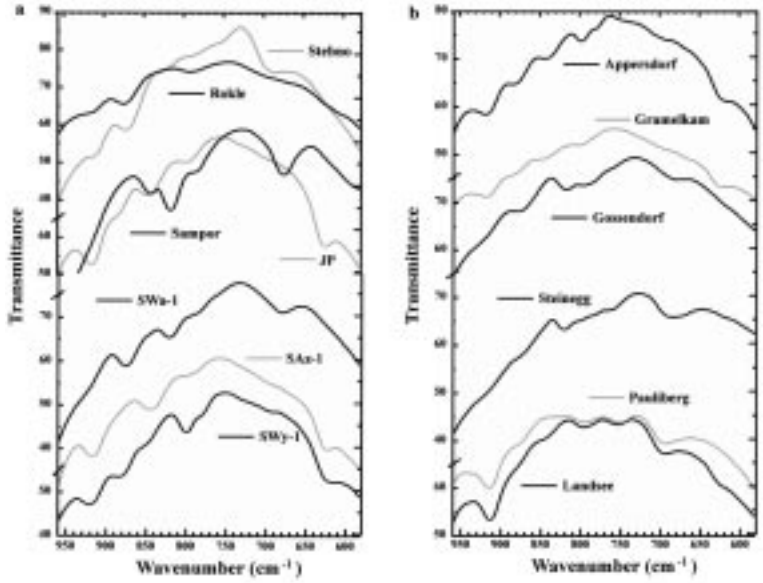

FIG. 2. Transmittance spectra of smectites from 580 to 960 cm^{-1}. (a) Samples from Stebno, Rokle, Sampor, Jelšový Potok (JP) and samples of SWa-1, SAz-1 and SWy-1; (b) samples from Appersdorf, Gramelkam, Gossendorf, Steinegg, Pauliberg and Landsee.

TABLE 3. Band assignments (cm^{-1}) for IR spectral features in smectites

JP	Sampor	Rokle	Stebno	SAz-1	SWa-1	SWy-1	Paul	Stein	Goss	Land	App	Gram	Assignment
(426)	430	(427)	(427)	(427)	427	(421)	428	(428)	427	(427)	(426)	(426)	Si-O bend
(443)				(443)				455	(456)				Si-O bend
470	(453)	469	465	469	467	470	469		471	469	470	471	Si-O-Si deformation
	491				(493)			496	495				Fe-O-Si deformation
521	(530)	520	515	520	(520)	525	532		(524)	529	522	522	Al-O-Si deformation
629				628		627				628	627	628	Al-smectite
	678				681			~675′	(687)				Fe-smectite
	(785)				(784)			(759)	(760)				MgFeOH bend
	819		(822)		818			822	820				FeFeOH bend
	845				(844)								FeFeOH deformation
845				841	(844)	(848)				843	841	844	AlMgOH bend
(883)		877	872		875	878	(876)	(875)	873	(877)	880	880	AlFeOH bend
915		916	912	915	(919)	916	914	(915)	(919)	913	916	915	AlAlOH bend (Sm or K)*
1039	1019	1036	1032	1032	1032	1048	1037	1027	1032	1033	1043	1043	Si-O stretch
	3567	~3600	~3600		3570			3546	3567	(3596)			OH stretch in Fe-smectite"
3629				3620		3634	3626			3623	3628	3629	OH stretch in Al-smectite"
	4005				(4005)			4000					Fe-smectite
	4165				(4170)			4200	(4165)				Fe-smectite
4105		4105		4095		4090					4090	4090	Al-smectite
	4380	(4370)	4375		4375			4355	4370				FeFeOH comb.
		4465	4475		4475		4470		(4465)				AlFeOH comb.
4525	(4575)	4530	4530	4520	(4575)	4535	4535		(4555)	4535	4530	4530	AlAlOH comb.
	6980				(6970)			6920	(6960)				FeFeOH overtone
7070		7070	7080	7060	7090	7090	7080		(7080)	7080	7080	7080	AlAlOH overtone

Band centres were determined using second derivatives except for the OH-stretching region; shoulder or weak features in the spectra are indicated by (), although these features appear as peaks in the second derivatives. Features due to admixtures are not included in this table, except for the AlAlOH bend which may be due to smectite* (Sm) or kaolinite (K). The ′ indicates that there is also another band ~700 cm^{-1} and the " indicates that this is an approximate band centre for multiple overlapping absorptions.

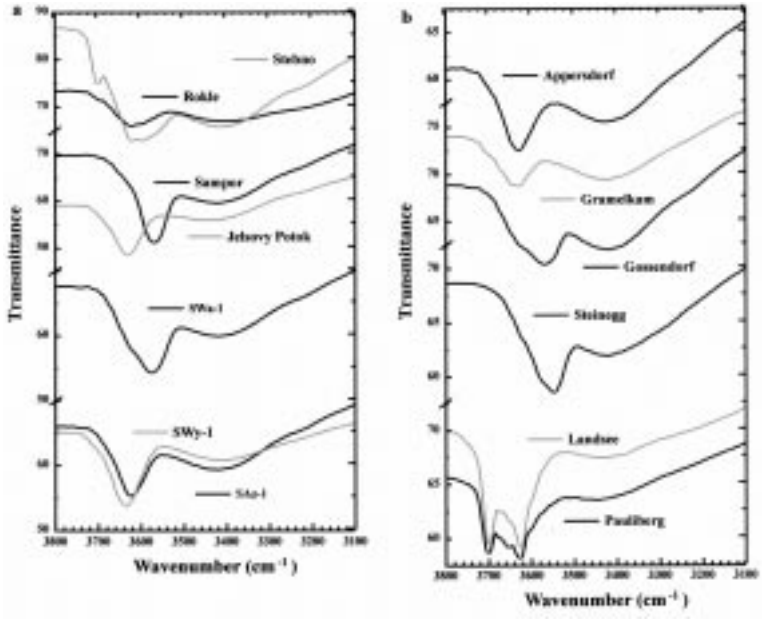

FIG. 3. Transmittance spectra of smectites from 3100 to 3800 cm^{-1}. (a) Samples from Stebno, Rokle, Sampor, Jelšový Potok and samples of SWa-1, SWy-1 and SAz-1, (b) samples from Appersdorf, Gramelkam, Gossendorf, Steinegg, Landsee and Pauliberg.

a band was reported for Sampor at 4155 cm^{-1}; however this band centre was determined from the reflectance spectra alone and includes a continuum factor (Bishop *et al*., 1999). Similar bands are found at 4200 and 4000 cm^{-1} in the spectra of Steinegg. Mid-IR spectra of Sampor and Steinegg also exhibit

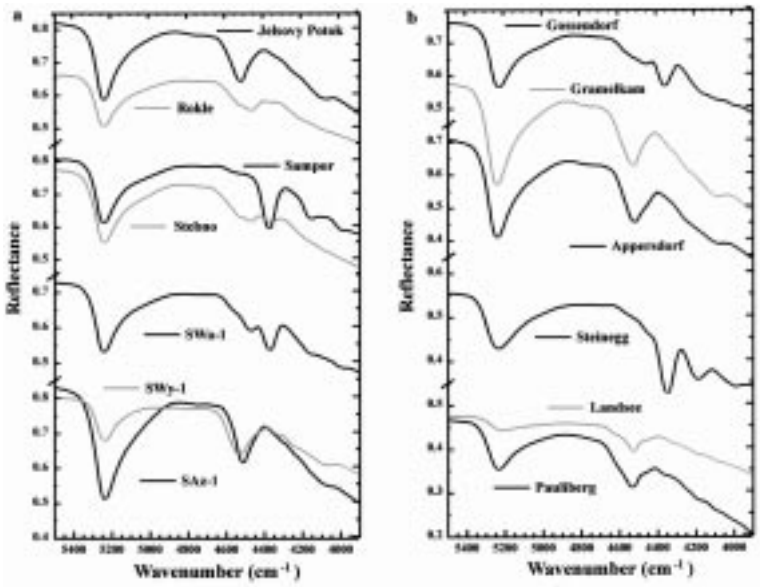

FIG. 4. Reflectance spectra of smectites from 3900 to 5500 cm^{-1}. (a) Samples from Jelšový Potok, Rokle, Sampor, Stebno and samples of SWa-1, SWy-1 and SAz-1; (b) samples from Gossendorf, Gramelkam, Appersdorf, Steinegg, Landsee and Pauliberg.

a strong band near 680 cm^{-1}. The ferruginous smectites SWa-1 and Gossendorf have weaker bands near 4170 and 680 cm^{-1}. These bands have been studied in more detail in a related study which suggests that the bands near 680 cm^{-1} are out-of-plane $OH_{\delta'}$ and the bands near 4170 cm^{-1} are due to $OH_{\nu+\delta'}$ for Fe-rich smectites with structural disorder due to tetrahedral and/or octahedral substition (Bishop *et al*., 2002, this issue). Analysis of the mid-IR transmittance spectra of nontronites shows that a strong 680 cm^{-1} band was observed for a nontronite from Manito that has particularly high tetrahedral substitution (Köster *et al*., 1999; Bishop *et al*., 2002). That study also suggests that the ~4100 and ~630 cm^{-1} bands may be due to $OH_{\nu+\delta'}$ and $OH_{\delta'}$ for Al-rich smectites with structural disorder due to tetrahedral and/or octahedral substitution. A previous study involving acid dissolution of montmorillonites noted that the ~630 cm^{-1} band disappeared as the octahedral sheet was eroded and assigned this band to an Al-O out-of-plane vibration (Madejová *et al*., 1998). The 680 cm^{-1} band of nontronites, assigned previously to an Fe-O out-of-plane vibration (Russell & Fraser, 1994), is often reported as a diagnostic band for nontronites. Further experiments are needed to verify final band assignments for these ~630 and ~680 cm^{-1} bands in montmorillonites and nontronites, respectively.

Characterization of Fe in smectites using optical spectra

Extended visible region reflectance spectra are shown in Fig. 5 and include bands due to excitation of the Fe. Sampor and Steinegg exhibit spectral bands here that are characteristic of nontronite. Second derivatives show band centres near 22200, 19300 and 15200 cm^{-1} for Sampor and near 22700, 19400 and 15100 cm^{-1} for Steinegg. The 22100 cm^{-1} band is assigned to tetrahedral Fe^{3+} from low-temperature Mössbauer studies (Bishop *et al*., 1999) and is much stronger for Sampor than Steinegg, indicating that Sampor may have more Fe^{3+} in tetrahedral sites than estimated in Table 2. Both SWa-1 and Gossendorf also have weak bands near 22500 cm^{-1} attributed to a small amount of tetrahedral Fe^{3+}. Besson & Drits (1997a,b) have suggested that smectites may have more tetrahedral substitution than is usually determined. Correlations between Fe^{3+} in tetrahedral sites and bands near 22500 and 680 cm^{-1} for more samples would help to explain these features. SWa-1, Gossendorf, Stebno and Rokle have bands centred near 19700 cm^{-1}, which is consistent with both Al and Fe^{3+} in octahedral sites. SWy-1, JP, Appersdorf, Gramelkam and Landsee exhibit weak bands near 20000−20600 and 15200−15400 cm^{-1}, which are

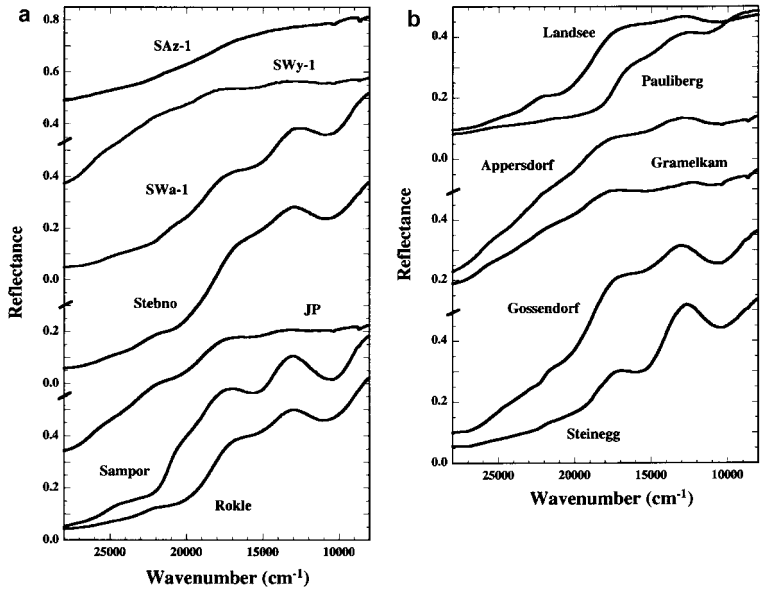

FIG. 5. Reflectance spectra of smectites from 28000 to 8000 cm^{-1}. (a) Samples of SAz-1, SWy-1, SWa-1, and from Stebno, Jelšový Potok (JP), Sampor and Rokle; (b) samples from Landsee, Pauliberg, Appersdorf, Gramelkam, Gossendorf and Steinegg.

characteristic of montmorillonite with a small amount of Fe^{3+} in octahedral sites (Bishop *et al*., 1999).

SUMMARY

Comparison of the NIR region OH-stretching overtones and OH-stretch-plus-bend combination bands with the mid-IR fundamental stretching and bending vibrations gives consistent results for a collection of smectites with different octahedral cation compositions.

The NIR bands are observed at ~4170 and 4000 cm^{-1} for nontronites and near 4100 cm^{-1} for montmorillonites with substantial tetrahedral and/or octahedral substitution. These bands are correlated with the mid-IR bands near 680 cm^{-1} for nontronite and near 630 cm^{-1} for montmorillonite.

The Sampor nontronite exhibits the strongest optical band for tetrahedral Fe^{3+} of the smectites in this study and also has the strongest band near 680 cm^{-1}. The smectites from Steinegg, Gossendorf and SWa-1 exhibit weaker optical tetrahedral Fe^{3+} bands and weaker bands near 680 cm^{-1}. These spectral features need to be studied for additional samples in order to determine trends and perhaps revise the methods used for assigning octahedral and tetrahedral cation compositions.

ACKNOWLEDGMENTS

The authors thank F. Ottner for supplying the Austrian and German samples from the collection of the Institute of Applied Geology, University of Agricultural Sciences, Vienna. Reflectance spectra were measured at RELAB, a multi-user, NASA-supported facility (NAG5-3871) at Brown University. Assistance from T. Hiroi with the bi-directional spectra is much appreciated, as well as financial support from the Slovak grant agency VEGA (grant 2/7202/00).

REFERENCES

Besson G. & Drits V.A. (1997a) Refined relationships between chemical composition of dioctahedral fine-grained micaceous minerals and their infrared spectra within the OH stretching region. Part I: Identification of the OH stretching bands. *Clays and Clay Minerals*, **45**, 158–169.

Besson G. & Drits V.A. (1997b) Refined relationships between chemical composition of dioctahedral fine-grained micaceous minerals and their infrared spectra within the OH stretching region. Part II: The main factors affecting OH vibrations and quantitative analysis. *Clays and Clay Minerals*, **45**, 170–183.

Bishop J.L., Pieters C.M. & Burns R.G. (1993) Reflectance and Mössbauer spectroscopy of ferrihydrite-montmorillonite assemblages as Mars soil analog materials. *Geochimica et Cosmochimica Acta*, **57**, 4583–4595.

Bishop J.L., Pieters C.M. & Edwards J.O. (1994) Infrared spectroscopic analyses on the nature of water in montmorillonite. *Clays and Clay Minerals*, **42**, 701–715.

Bishop J.L., Murad E., Madejová J., Komadel P., Wagner U. & Scheinost A. (1999) Visible, Mössbauer and infrared spectroscopy of dioctahedral smectites: Structural analyses of the Fe-bearing smectites Sampor, SWy-1 and SWa-1. Pp. 413–419 in: *11th International Clay Conference, June, 1997*.

Bishop J.L., Froeschl H., Lougear A., Newton J., Körner W., Koeberl C., Doran P. & Trautwein A.X. (2001) Mineralogical and geochemical analyses of Antarctic sediments: A reflectance and Mössbauer spectroscopy study with applications for remote sensing on Mars. *Geochimica Cosmochimica Acta*, **65**, 2875–2897.

Bishop J.L., Murad E. & Dyar M.D. (2002) The influence of octahedral and tetrahedral cation substitution on the structure of smectites and serpentines as observed through infrared spectroscopy. *Clay Minerals*, **37**, 617–628.

Breen C., Madejová J. & Komadel P. (1995) Characterisation of moderately acid-treated, size-fractionated montmorillonites using IR and MAS NMR spectroscopy and thermal analysis. *Journal of Material Chemistry*, **5**, 469–474.

Cariati F., Erre L., Gessa C., Micera G. & Piu P. (1981) Water molecules and hydroxyl groups in montmorillonites as studied by near infrared spectroscopy. *Clays and Clay Minerals*, **29**, 157–159.

Číčel B. & Komadel P. (1994) Structural formulae of layer silicates. Pp. 114–136 in: *Quantitative Methods in Soil Mineralogy* (J.E. Amonette & L.W. Zelazny, editors). Soil Science Society of America, Madison, Wisconsin, USA.

Číčel B., Komadel P., Bednáriková E. & Madejová J. (1992a) Mineralogical composition and distribution of Si, Al, Fe, Mg and Ca in the fine fractions of some Czech and Slovak bentonites. *Geologica Carpathica – Clays*, **1**, 3–7.

Číčel B., Komadel P., Lego S., Madejová J. & Vicková L. (1992b) Iron-rich beidellite in bentonite from Stebno. *Geologica Carpathica–Clays*, **2**, 121–124.

Clark R.N., King T.V.V., Klejwa M. & Swayze G.A. (1990) High spectral resolution reflectance spectroscopy of minerals. *Journal of Geophysical Research*,

95, 12653–12680.

Cornell R.M. & Schwertmann U. (1996) *The Iron Oxides*. VCH, New York.

Farmer V.C. (1974) The layer silicates. Pp. 331–363 in: *The Infrared Spectra of Minerals* (V.C. Farmer, editor). Monograph **4**, The Mineralogical Society, London.

Goodman B.A., Russell J.D., Fraser A.R. & Woodhams F.W.D. (1976) A Mössbauer and IR spectroscopy study of the structure of nontronite. *Clays and Clay Minerals*, **24**, 53–59.

Köster H.M., Ehrlicher U., Gilg H.A., Jordan R., Murad E. & Onnich K. (1999) Mineralogical and chemical characteristics of five nontronites and Fe-rich smectites. *Clay Minerals*, **34**, 579–599.

Madejová J., Komadel P. & Čičel B. (1994) Infrared study of octahedral site populations in smectites. *Clay Minerals*, **29**, 319–326.

Madejová J., Budják J., Janek M. & Komadel P. (1998) Comparative FT-IR study of structural modifications during acid treatment of dioctahedral smectites and hectorite. *Spectrochimica Acta, Part A*, **54**, 1397–1406.

Russell J.D. & Fraser A.R. (1994) Infrared methods. Pp. 11–67 in: *Clay Mineralogy: Spectroscopic and Chemical Determinative Methods* (M.J. Wilson, editor). Chapman & Hall, London.

Schwertmann U. & Cornell R.M. (2000) *Iron Oxides in the Laboratory*. Wiley-VCH, New York.

Stubican V. & Roy R. (1961) A new approach to the assignment of infrared absorption bands in layer silicates. *Zeitschrift für Kristallographie*, **115**, 200–214.

Vantelon D., Pelletier M., Barres O., Thomas F. & Michot L.J. (2001) Fe, Mg and Al distribution in the octahedral sheet of montmorillonites. An infrared study in the OH-bending region. *Clay Minerals*, **36**, 369–379.